Diffraction optical tomography using a quantitative phase imaging unit

Kyoohyun Kim[1,†], **Zahid Yaqoob**[2,†], **KyeoReh Lee**[1], **Jeon Woong Kang**[2], **Youngwoon Choi**[2], **Poorya Hosseini**[2,3,4], **Peter T. C. So**[2,3,4,5], and **YongKeun Park**[1,*]

[1]Department of Physics, Korea Advanced Institutes of Science and Technology, Daejeon 305-701, South Korea

[2]Laser Biomedical Research Center, Massachusetts Institute of Technology, Cambridge, Massachusetts 02139, USA

[3]Department of Mechanical Engineering, Massachusetts Institute of Technology, Cambridge, Massachusetts 02139, USA

[4]Department of Biological Engineering, Massachusetts Institute of Technology, Cambridge, Massachusetts 02139, USA

Abstract

A simple and practical method to measure three-dimensional (3-D) refractive index (RI) distributions of biological cells is presented. A common-path self-reference interferometry consisting of a compact set of polarizers is attached to a conventional inverted microscope equipped with a beam scanning unit, which can precisely measure multiple 2-D holograms of a sample with high phase stability for various illumination angles, from which accurate 3-D optical diffraction tomograms of the sample can be reconstructed. 3-D RI tomograms of nonbiological samples such as polystyrene microspheres, as well as biological samples including human red blood cells and breast cancer cells, are presented.

Refractive index (RI) distribution is an intrinsic optical property that can provide valuable information about a sample. For biological cells and tissues, the knowledge of RI distribution can provide structural, as well as chemical composition since it is directly related to the protein concentrations [1]. Thus, the ability to measure three-dimensional (3-D) RI distribution of biological samples provides a unique advantageous way to investigate pathophysiological conditions at single cell level. More specifically, it can be used to study morphological changes in human red blood cells (RBCs) in response of malaria-infection [2–4], in shear flow [5], and dry mass changes of chromosomes during mitosis [6].

*Corresponding author: yk.park@kaist.ac.kr.
5ptso@mit.edu
†These authors equally contributed to this work.

Recently, several optical techniques have been introduced to measure 3-D shape or RI distribution in biological cells. For instance, digital holography based configurations have been used to provide 3-D shape or morphology/average RI [7–10], whereas optical diffraction tomography based approaches have led to 3-D RI mapping [11–20]. For the latter case, it is customary to acquire multiple 2-D complex optical fields with sample information using interferometry for various angles of illumination. The 3-D RI distribution of the sample is then numerically reconstructed via appropriate tomographic algorithms [21–24]. While 3-D RI mapping provides unique advantages such as noninvasiveness, label-free capability, and quantitative imaging, its translation for different applications has been limited mainly because of the complexity of the optical system design. Typical optical tomographic instruments involve complicated setups requiring careful alignment. Furthermore, the setup is typically not compatible with an existing optical microscope.

More recently, various microscopic techniques have been proposed to simplify the measurement of 3-D RI distribution of biological samples using conventional microscopes, including spatial light interference tomography (SLIT) [25], quadriwave lateral shearing interferometer (QWLSI) [26], and techniques based on the transport of intensity equation (TIE) [27]. However, those techniques still require expensive optical components such as a spatial light modulator, precise alignment and time-consuming data acquisition processes, and heavy computation for tomogram reconstruction.

In this Letter, we propose and experimentally demonstrate a simple and practical optical approach for tomographic phase microscopy, referred to as diffraction optical tomography unit (DOTU). DOTU measures the 3-D RI map of a sample by employing an angle scanning unit for varying illumination in the quantitative phase imaging unit (QPIU) [28]. The present approach is simple and effective, and is readily compatible to an existing optical microscope.

DOTU consists of two parts: an illumination scanning part and a self-reference interferometer, as shown in Fig. 1(a). A collimated beam from a fiber-coupled diode laser (λ = 635 nm, 5 mW, Lasiris Mini, Coherent Inc.) is linearly polarized, and then reduced in size using a tube lens (f = 175 mm) and a condenser lens [UPLSAPO 60×, water immersion, numerical aperture (NA) = 1.2, Olympus Inc.]. The angle of the illumination beam is tilted by using a dual-axis galvano scanner (3 mm on 6200H, Cambridge Technology) located at a plane conjugate to the sample plane to illuminate a sample with various angles. The illumination beam is spirally scanned in 150 different angles, which sparsely span the NA of the condenser.

The diffracted beam from a sample is collected by an objective lens (Fluar 100×, oil immersion, NA = 1.3, Carl Zeiss AG) and a tube lens (f = 200 mm) in a conventional inverted microscope (TE 2000-E, Nikon Inc.). Since the reference focal length of the Zeiss objective lens (165 mm) is different from that of the Nikon objective lens (200 mm), a sample image is further magnified such that the total magnification is approximately 120×. Furthermore, a QPIU is employed [28] to measure multiple 2-D quantitative phase images illuminated with plane waves at various angles. A QPIU is a unit consisting of a series of

polarization sensitive optics, which generates an interferogram at the image plane using spatially-shifted wavefronts.

In a nutshell, the QPIU utilizes a Rochon polarizer and a linear polarizer, which makes the system more compact and effective, compared to the previous work [28]. A Rochon polarizer (MgF_2, Edmund Optics, Inc.) placed at the image plane of the microscope splits the beam into two, the ordinary and extraordinary beam with different propagation directions. After passing a polarizer, two beams interfere at the image plane and generate a spatially modulated hologram, which is recorded by a charge-coupled device (CCD) camera (FL3-U3-13Y3M-C, Point Grey Inc.). The fringe period is defined entirely by the Rochon prism selected, and does not change for different angles of illumination. The angle of illumination in the sample plane was therefore experimentally calibrated using a Mach–Zehnder interferometer. The 2-D Fourier spectra of illumination beams are depicted as red circles in Fig. 1(b). It shows that the scanning range of the illumination covers up to 64°, which is compatible to the maximum acceptance angle of the condenser lens limited by the NA [the red dotted circle in Fig. 1(b)].

A complex optical field of the sample, consisting of amplitude and phase delay images, is extracted from the measured holograms using a field retrieval algorithm based on Fourier transform [29,30]. Retrieved complex optical fields obtained with various illumination angles are used to reconstruct the 3-D RI distribution of the sample via optical diffraction tomography algorithm [23]. More specifically, 2-D Fourier spectra of retrieved optical fields from various illumination angles are mapped onto an Ewald sphere in a 3-D Fourier space according to the Fourier diffraction theorem [31]. Since the maximum illumination angle is limited by the NA of the objective lens, a 3-D Fourier space has missing information causing shape distortion in the reconstructed tomogram along the axial direction. We have used an iterative non-negativity constraint algorithm [23] to fill the missing information. The theoretical lateral and axial resolution of the optical diffraction tomogram is 122 and 432 nm, respectively, which was calculated from the maximum range of the Fourier spectra [32]. The lateral and axial resolution are experimentally measured as 276.5 and 1.23 μm, respectively, which as calculated by analyzing the edge of the reconstructed tomograms of polystyrene beads. The spatial resolution of optical diffraction tomography can be further enhanced using spatial deconvolution [15].

Compared with the reported QPIU [28], we have utilized a Rochon polarizer in DOTU (rather than a Wollaston prism) because a Rochon polarizer does not tilt the ordinary beam from the optic axis and only an extraordinary beam is deviated. As a result, the wavefront of the ordinary beam stays parallel to the camera plane such that the image quality is not degraded. The distance between the Rochon polarizer and the camera is 150 mm to achieve desired lateral shift between the ordinary and extraordinary beams. In our setup, we achieve this condition by utilizing additional 4-f relay lenses at the output of the Nikon microscope, as shown in Fig. 1(a). In turn, this allows us to place the Rochon polarizer in an intermediate plane between the camera and the output port of the microscope. This strategy, however, is not a necessary requirement for DOTU. In fact, one may use a Rochon polarizer of a larger separation angle (α-BBO: 8.14°, YVO_4:10.93° at λ = 635 nm) that should allow placing the Rochon polarizer within a limited space between the microscope body and camera plane.

The common-path design of DOTU also enables dynamic phase measurements with high stability, which is crucial for studying the dynamics of cells and tissues [33–37]. To demonstrate the high phase stability of the system, we measured 250 time-lapse phase maps of a human RBC for 2.08 seconds at a frame rate of 120 Hz (Fig. 2). The root-mean squared displacement map of dynamic phase images of the RBC [see Fig. 2(b)] clearly demonstrates the high phase sensitivity of the present method. Measured mean and root-mean squared displacement values at the outer convex region [green dot in Figs. 2(a) and 2(b)] of the RBC are 2.83 μm and 80.9 nm, respectively, whereas the values at the dimple region (blue dot) are 1.32 μm and 56.3 nm. The root-mean squared displacement value in the background region (red dot) is 12.0 nm. These measurements were obtained by the DOTU setup implemented on an optical table to which anti-vibration air flotation is not applied. Those values are in good agreement with the previous work employing common-path interferometry [38,39].

To demonstrate 3-D tomographic imaging capability of DOTU, we measured RI distributions of several samples, including microspheres and live biological cells. We first measured a polystyrene microsphere with a diameter of 6 μm ($n = 1.587$ at $\lambda = 635$ nm, Polyscience Inc.) immersed in index matching oil ($n = 1.56$, Cargille Laboratories). In total, 150 2-D holograms of the sample were measured by scanning the illumination beam within an angle range limited by the NA of the condenser lens. Next, a 3-D RI tomogram of the microsphere was reconstructed by employing a diffraction tomography algorithm [3]. The overall 3-D morphology and the mean RI value of the beads are in good agreement with the manufacturer's specification [Fig. 3(a)].

Subsequently, we measured 3-D RI tomograms of individual biological cells. Reconstructed 3-D RI distribution of a human RBC from a healthy donor exhibits a characteristic discoid shape of healthy RBCs [Fig. 3(b)]. The cross-sectional slices in the y–z and x–z planes clearly show a dimple at the center of the RBC. Hemoglobin (Hb) concentration inside RBCs can be directly calculated from the reconstructed RI value of RBCs with *a priori* knowledge on the RI increment value [40,41] ($dn/dc = 0.144$ ml/g at $\lambda = 635$ nm for oxygenated Hb). The calculated Hb concentration of the measured RBC is 33.41 g/dl, which is within the normal physiological range. In addition, the 3-D RI tomogram of a breast cancer cell (MDA-MB-435S, human breast ductal carcinoma, HTB-129, ATCC) was measured [Fig. 3(c)], which shows complicated internal structures of the cell.

In conclusion, we present DOTU, a simple but powerful optical method, which can add tomographic imaging capability to a standard microscope. By adding a beam scanner at the illumination side and inserting a Rochon prism and a polarizer at the output port, complex optical field images of a sample can be quantitatively measured for various illumination angles, leading to 3-D RI maps of the sample under observation. Since DOTU is based on common-path interferometry, it measures optical fields with high precision and high phase stability. Furthermore, this common-path interferometry is realized only using two optical components (a Rochon polarizer and a linear polarizer used as an analyzer), which can be readily incorporated into an existing microscope.

Although RI provides intrinsic quantitative optical imaging contrast of biological cells and tissues, RI itself does not provide molecular specificity to determine specific proteins inside samples. Nonetheless, the molecular specificity can be addressed in DOTU by combining fluorescence imaging modality or exploiting optical phase dispersion [42–46] in the future.

We believe that the presented technique can be used as an add-on module in conventional microscopes for investigating 3D morphological and chemical characteristics of biological samples, and anticipate that this simple approach will allow immediate application of diffraction tomography to the field of biophotonics.

Acknowledgments

References

1. Barer R. Nature. 1952; 169:366. [PubMed: 14919571]

2. Park YK, Diez-Silva M, Popescu G, Lykotrafitis G, Choi WS, Feld MS, Suresh S. Proc Natl Acad Sci USA. 2008; 105:13730. [PubMed: 18772382]

3. Kim K, Yoon HO, Diez-Silva M, Dao M, Dasari R, Park YK. J Biomed Opt. 2014; 19:011005. [PubMed: 23797986]

4. Chandramohanadas R, Park Y, Lui L, Li A, Quinn D, Liew K, Diez-Silva M, Sung Y, Dao M, Lim CT, Preiser PR, Suresh S. PLoS One. 2011; 6:e20869. [PubMed: 21698115]

5. Kim K, Kim KS, Park H, Ye JC, Park Y. Opt Express. 2013; 21:32269. [PubMed: 24514820]

6. Sung Y, Choi W, Lue N, Dasari RR, Yaqoob Z. PLoS ONE. 2012; 7:e49502. [PubMed: 23166689]

7. Rappaz B, Marquet P, Cuche E, Emery Y, Depeursinge C, Magistretti PJ. Opt Express. 2005; 13:9361. [PubMed: 19503137]

8. Cardenas N, Mohanty SK. Appl Phys Lett. 2013; 103:013703.

9. Merola F, Miccio L, Memmolo P, Di Caprio G, Galli A, Puglisi R, Balduzzi D, Coppola G, Netti P, Ferraro P. Lab Chip. 2013; 13:4512. [PubMed: 24129638]

10. Memmolo P, Miccio L, Merola F, Gennari O, Netti PA, Ferraro P. Cytometry Part A. 2014

11. Popescu, G. Quantitative Phase Imaging of Cells and Tissues. McGraw-Hill; 2011.

12. Lee K, Kim K, Jung J, Heo J, Cho S, Lee S, Chang G, Jo Y, Park H, Park Y. Sensors. 2013; 13:4170. [PubMed: 23539026]

13. Sung Y, Lue N, Hamza B, Martel J, Irimia D, Dasari RR, Choi W, Yaqoob Z, So P. Phys Rev Appl. 2014; 1:014002. [PubMed: 25419536]

14. Kim T, Zhou RJ, Mir M, Babacan SD, Carney PS, Goddard LL, Popescu G. Nat Photonics. 2014; 8:256.

15. Cotte Y, Toy F, Jourdain P, Pavillon N, Boss D, Magistretti P, Marquet P, Depeursinge C. Nat Photonics. 2013; 7:113.

16. Hsu WC, Su JW, Tseng TY, Sung KB. Opt Lett. 2014; 39:2210. [PubMed: 24686713]

17. Kim Y, Shim H, Kim K, Park H, Heo JH, Yoon J, Choi C, Jang S, Park Y. Opt Express. 2014; 22:10398. [PubMed: 24921741]

18. Kim MK. SPIE Rev. 2010; 1:018005.

19. Kühn J, Montfort F, Colomb T, Rappaz B, Moratal C, Pavillon N, Marquet P, Depeursinge C. Opt Lett. 2009; 34:653. [PubMed: 19252582]

20. Fiolka R, Wicker K, Heintzmann R, Stemmer A. Opt Express. 2009; 17:12407. [PubMed: 19654642]

21. Charriere F, Marian A, Montfort F, Kuehn J, Colomb T, Cuche E, Marquet P, Depeursinge C. Opt Lett. 2006; 31:178. [PubMed: 16441022]

22. Choi W, Fang-Yen C, Badizadegan K, Oh S, Lue N, Dasari RR, Feld MS. Nat Methods. 2007; 4:717. [PubMed: 17694065]

23. Sung Y, Choi W, Fang-Yen C, Badizadegan K, Dasari RR, Feld MS. Opt Express. 2009; 17:266. [PubMed: 19129896]

24. Kou SS, Sheppard CJR. Opt Lett. 2008; 33:2362. [PubMed: 18923623]

25. Wang Z, Marks DL, Carney PS, Millet LJ, Gillette MU, Mihi A, Braun PV, Shen Z, Prasanth SG, Popescu G. Opt Express. 2011; 19:19907. [PubMed: 21996999]

26. Bon P, Aknoun S, Monneret S, Wattellier B. Opt Express. 2014; 22:8654. [PubMed: 24718236]

27. Phillips KG, Jacques SL, McCarty OJ. Phys Rev Lett. 2012; 109:118105. [PubMed: 23005682]

28. Lee K, Park Y. Opt Lett. 2014; 39:3630. [PubMed: 24978554]

29. Takeda M, Ina H, Kobayashi S. J Opt Soc Am. 1982; 72:156.

30. Cuche E, Marquet P, Depeursinge C. Appl Opt. 2000; 39:4070. [PubMed: 18349988]

31. Wolf E. Opt Commun. 1969; 1:153.

32. Lauer V. J Microsc. 2002; 205:165. [PubMed: 11879431]

33. Park Y, Best CA, Badizadegan K, Dasari RR, Feld MS, Kuriabova T, Henle ML, Levine AJ, Popescu G. Proc Natl Acad Sci USA. 2010; 107:6731. [PubMed: 20351261]

34. Wang R, Ding HF, Mir M, Tangella K, Popescu G. Biomed Opt Express. 2011; 2:485. [PubMed: 21412454]

35. Byun HS, Hillman TR, Higgins JM, Diez-Silva M, Peng Z, Dao M, Dasari RR, Suresh S, Park YK. Acta Biomater. 2012; 8:4130. [PubMed: 22820310]

36. Shaked NT, Zhu Y, Rinehart MT, Wax A. Opt Express. 2009; 17:15585. [PubMed: 19724557]

37. Kim Y, Shim H, Kim K, Park H, Jang S, Park Y. Sci Rep. 2014; 4:6659. [PubMed: 25322756]

38. Park YK, Best CA, Auth T, Gov NS, Safran SA, Popescu G, Suresh S, Feld MS. Proc Natl Acad Sci USA. 2010; 107:1289. [PubMed: 20080583]

39. Kim, Y.; Kim, K.; Park, Y. Blood Cell—An Overview of Studies in Hematology. Moschandreou, TE., editor. INTECH; 2012. p. 167-194.

40. Friebel M, Meinke M. Appl Opt. 2006; 45:2838. [PubMed: 16633438]

41. Zhernovaya O, Sydoruk O, Tuchin V, Douplik A. Phys Med Biol. 2011; 56:4013. [PubMed: 21677368]

42. Fu D, Choi W, Sung YJ, Yaqoob Z, Dasari RR, Feld M. Biomed Opt Express. 2010; 1:347. [PubMed: 21113234]

43. Jang Y, Jang J, Park Y. Opt Express. 2012; 20:9673. [PubMed: 22535058]

44. Lue N, Kang JW, Hillman TR, Dasari RR, Yaqoob Z. Appl Phys Lett. 2012; 101:084101.

45. Rinehart M, Zhu YZ, Wax A. Biomed Opt Express. 2012; 3:958. [PubMed: 22567588]

46. Jung JH, Jang J, Park Y. Anal Chem. 2013; 85:10519. [PubMed: 24079982]
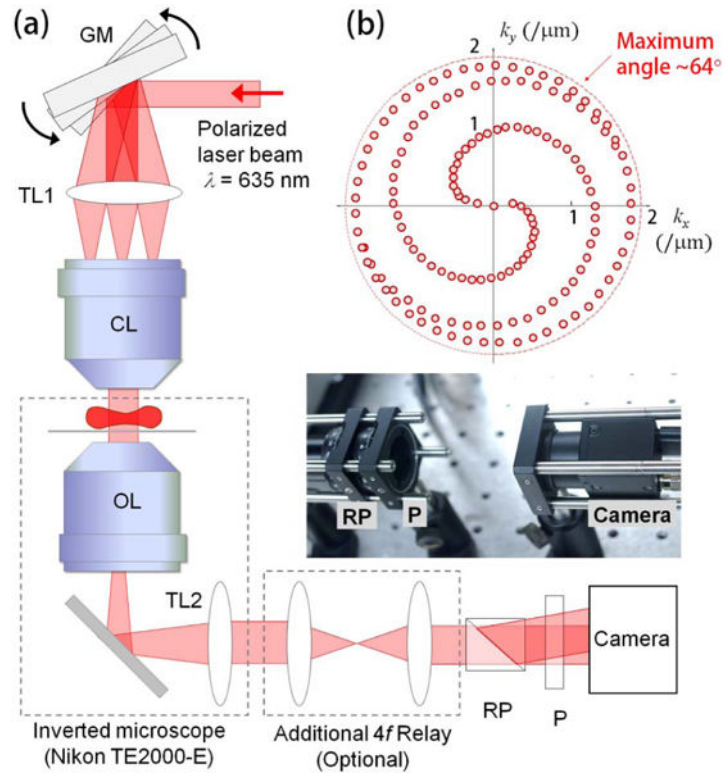
Fig. 1.
(a) Experimental setup for optical tomographic imaging unit. GM, galvanomirror; CL, condenser lens; OL, objective lens; TL, tube lens; RP, Rochon polarizer; and P, polarizer. (b) Angles of spirally scanned incident beam at the sample plane in spatial frequency domain. The red circle indicates the maximum angle limited by the numerical aperture of condenser lens ($NA = 1.2$, water immersion)
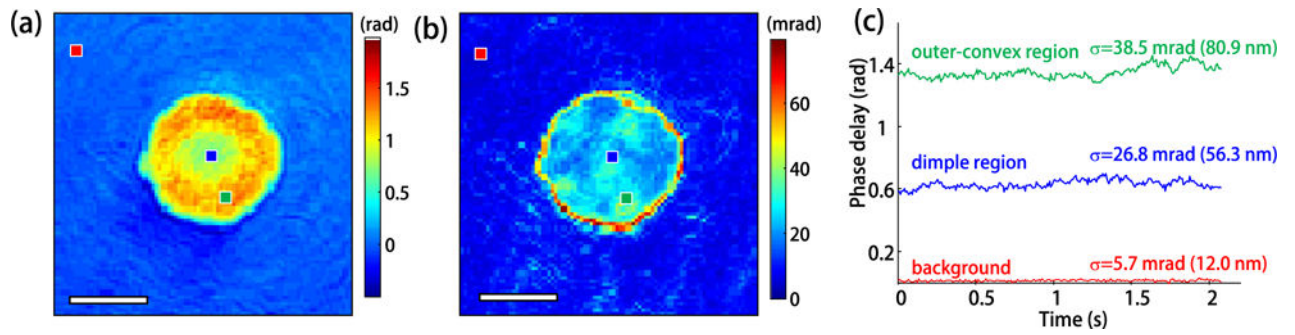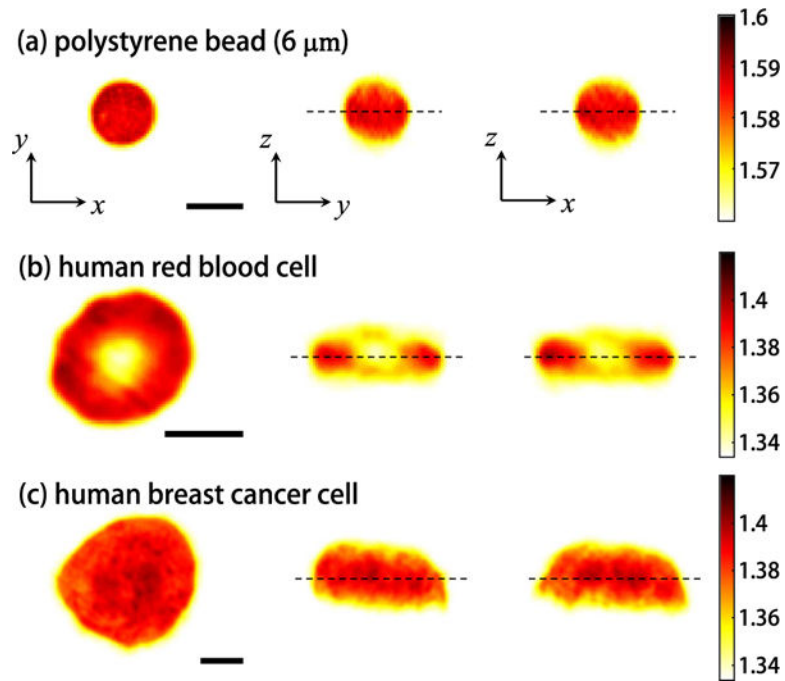
Fig. 2.
Dynamic quantitative phase delay measurements in a healthy red blood cell. (a) Mean phase delay and (b) root mean squared phase delay of a red blood cell. Scale bar indicated 5 µm. (c) Temporal fluctuation of phase delay at outer-convex region (green), dimple region (blue), and background (red) marked in (a) and (b), respectively.

Fig. 3.
Cross-sectional slices of a reconstructed refractive index tomogram of (a) a 6-µm polystyrene bead, (b) human red blood cell, and (c) breast cancer cell in the *x–y* (left panel), *y–z* (center panel), and *x–z* (right panel) planes, respectively. Dotted lines correspond to focal planes. Each scale bar indicates 5 µm